Neuroretinal Dysfunction in Patients Affected by Neurofibromatosis Type 1

Antonietta Moramarco
  Sapienza University of Rome
Luca Lucchino
  Sapienza University of Rome
Fabiana Mallone
  Sapienza University of Rome
Michela Marcelli
  Sapienza University of Rome
Ludovico Alisi
  Sapienza University of Rome
Vincenzo Roberti
  Sapienza University of Rome
Sandra Giustini
  Sapienza University of Rome
ALESSANDRO LAMBIASE (✉ alessandro.lambiase@uniroma1.it)
  Sapienza University of Rome
Marcella Nebbioso
  Sapienza University of Rome

Research Article

Abstract

The aim of the study was to examine neuroretinal function by using the mfERG test in patients with neurofibromatosis type 1 (NF1) without optic pathway gliomas (OPGs). This study was conducted on 35 patients (35 eyes) with NF1 and 30 healthy subjects (30 eyes) for the control group. Each subject underwent a complete ophthalmological examination including multifocal electroretinography (mfERG). 1.5-Tesla magnetic resonance imaging (MRI) scan of the brain was performed in NF1 patients to assess the presence of OPGs. All participants were recruited having a best corrected visual acuity (BCVA) of no less than 20/20 in each eye. The amplitude and implicit time of the P1 wave (first-order Kernel component) were evaluated on mfERG. Data analysis was carried out in the two central degrees and in the four quadrants from two to 25 degrees of visual field. Statistically significant results were obtained for the P1 wave amplitudes in the 4 quadrants in NF1 patients compared to healthy subjects, while the reduction was not significant in the 2 central degrees. A statistically significant difference was observed among the P1 wave amplitudes as recorded in the 4 quadrants within the NF1 group, with lower amplitudes in the nasal quadrants. No differences in the implicit times were recorded in the 4 quadrants and in the 2 central degrees as compared between NF1 patients and controls.

The present study demonstrates impaired neuroretinal function in NF1 patients. Altered intracellular signal transduction due to abnormal neurofibromin-mediated cyclic adenosine monophosphate (cAMP) generation, could be involved. Our results suggest a possible use of mfERG as subclinical retinal damage indicator with a potential utility in clinical practice for the follow-up of NF1 patients.

Key Messages

- Neurofibromatosis type 1 (NF1) is an autosomal dominant disorder with multiple eye involvement. Neuroretinal function in NF1 patients is a relatively unknown topic.
- This is the first study to evaluate neuroretinal function in NF1 patients in the absence of optic pathway gliomas (OPGs).
- In NF1 patients with normal or corrected to normal visual acuity and no OPGs, there is a decrease in neuroretinal function as expressed in a reduced amplitude of the P1-wave between 2 and 25 central retinal degrees on multifocal electroretinography (mfERG).
- Impaired intracellular signal transduction due to abnormal neurofibromin-mediated cyclic adenosine monophosphate (cAMP) generation may be involved.
- MfERG could be used as a subclinical retinal damage indicator in the follow-up of NF1 patients.

Introduction

Neurofibromatosis type 1 (NF1), also known as Von Recklinghausen disease, is a rare genetic disorder that is transmitted in an autosomal dominant fashion, with complete penetrance and variable expressivity.

It is caused by a mutation in the NF1 gene located on chromosome 17q11.2 which encodes for neurofibromin, a tumor suppressive protein involved in RAS signaling pathways [1,2]. The disease is 50% sporadic or inherited, and it occurs with an estimated frequency of approximately 1:2500-1:3500, without any known gender or ethnic predilections. Individuals with NF1 are prone to the development of both malignant and benign nervous system tumors, skeletal dysplasia, and skin abnormalities [1,3]. The eye and ocular adnexa are frequently involved in NF1. Some ocular manifestations of NF1 including optic pathway gliomas (OPGs), iris Lisch nodules, orbital and eyelid neurofibromas, eyelid café-au-lait spots, are diagnostic of the disease. Additional ocular features have recently been characterized and are not currently diagnostic for NF1, including choroidal nodules, retinal microvascular abnormalities, and hyperpigmented spots of the fundus oculi [4–7]. The presence of electrophysiological changes in NF1 was previously investigated on visual evoked potentials (VEPs) in patients with related OPGs. Notably, abnormal visual evoked responses allowed for early detection of optic gliomas in NF1 and earlier intervention prior to significant visual loss [8,9]. However, electrophysiological abnormalities were also reported in the absence of optic gliomas in NF1 patients. Specifically, abnormal VEPs were described in NF1 regardless of the presence of gliomas of the optic pathways or of the brain. These findings were ascribed to a primary abnormality of visual processing in NF1 [10]. Similarly, our group demonstrated subclinical impairment in the conduction of visual stimuli in patients with NF1 and absence of any condition affecting the optical pathways, as assessed on VEPs and frequency-doubling technology (FDT) campimetry [11]. Unlike the optical pathways, electrophysiological evaluation of the neuroretina

as an earlier indicator of the damage to the axons forming the optic nerve in NF1 has scarcely been characterized. Experimental studies on murine models of NF-1 and OPGs showed progressive loss by apoptosis of retinal ganglion cells (RGCs) occurring in early phases of OPG development [12]. In accordance, inner retinal dysfunction was reported in a subgroup of patients with NF1 and OPGs on electroretinogram (ERG) examination [13]. However, neuroretinal function in NF1 in the absence of OPGs is a relatively unknown topic. In the present study, we assessed neuroretinal function by using the multifocal electroretinography (mfERG). The mfERG is a technique that allows local ERG responses to be recorded simultaneously from many regions of the retina [14]. Specifically, through the simultaneous stimulation of multiple retinal areas and recording of each response independently, mfERG provides a topographic measure of retinal electrophysiological activity in the central 25 degrees retina. Therefore, the aim of this study was to examine retinal function by using the mfERG test in NF1 patients without OPGs and any other disorder of the visual pathways.

Results

The normal distribution of data was assessed using the D'Agostino-Pearson test. Statistical significance was determined by Fisher's exact test for qualitative variables. Comparisons between groups were performed by Student t-test and Mann-Whitney test, respectively for normally and not normally distributed data. Comparisons between more than 2 groups were performed by repeated measures ANOVA test and Friedman test, respectively for normally and not normally distributed data. A value of $p \leq 0.05$ was considered statistically significant. Statistical analysis was performed using Graph Pad vers. 8.0.2 and IBM® SPSS® Statistics version 24.0 (IBM Corp., Armonk, NY, USA) on the Windows 10 Home edition platform. v22 (IBM SPSS Statistics, IBM®, IL, USA).

Five eyes in NF1 group and 5 eyes in the HC group were excluded due to excessive signal-to-noise ratio on mfERG. Therefore, the final samples consisted of 30 patients (18 females, 12 males), mean age 30.8 ± 10.47 standard deviation (SD), for a total of 30 eyes examined; whereas HC group consisted of 25 subjects (14 females, 11 males) mean age 33.76 ± 6.1 SD, for a total of 25 eyes examined. There were no significant differences between groups in terms of age and gender (Table 1). The best corrected visual acuity (BCVA) was 20/20 in all patients, as per inclusion criteria. Lisch nodules were detected in 25 eyes (83,3%) of NF1 patients and none of the HC group. Intraocular pressure was within normal limits in the totality of patients. No pathologic alterations were identifiable at mydriatic indirect fundus biomicroscopy exam in both the NF1 and HC group. At cross-sectional SD-OCT and NIR-OCT evaluation, 28 eyes out of 30 (93,3%) in the NF1 group showed the presence of choroidal nodules variously distributed to the posterior pole, whereas no choroidal abnormalities were recognizable in the HC group [19–21]. At MRI evaluation, no patient had optic nerve gliomas or other lesions involving the optic pathways. The analysis of the trace arrays showed no differences in the uniformity of the waveforms between NF1 patients and HC subjects. NF1 patients had significantly lower values of the P1-wave amplitudes in all of the 4 quadrants when compared to HC (Table 1, Figs. 1 and 2), whereas, there were no differences of the P1-wave amplitude in the 2 central degrees between the groups. In addition, a statistically significant difference was observed among the P1 wave amplitudes as recorded in the 4 quadrants within the NF1 group. Specifically, lower amplitudes were recorded in the nasal quadrants (Table 2, Fig. 3). Similar results were obtained for the HCs as summarized in Table 2. Table 2 shows the comparison analyses among the P1-wave amplitudes as evaluated in the 4 quadrants in NF1 patients and HC subjects. No statistically significant differences were observed in the absolute values of implicit time between NF1 patients and HCs (Table 1). Moreover, no differences were observed in the implicit times as recorded in the 4 quadrants within the NF1 group and among HCs.

Table 1

Table 1

Baseline characteristics of neurofibromatosis type 1 (NF1) patients and healthy controls (HCs) and comparisons of the P1 wave amplitudes and implicit times in the 4 quadrants on multifocal electroretinography (mfERG) between the two groups. SD: standard deviation; SN: supero-nasal; ST: supero-temporal; IN: infero-nasal; IT: infero-temporal; 4Q: average of the 4 quadrants.

	NF1 (mean ± SD)	HC (mean ± SD)	p value
Age	30.8 ± 10.47	33.76 ± 6.1	0.217[a]
Gender			
Male	12	11	0.790[b]
Female	18	14	
P1 Amplitude, nV/deg²			
Central	102.03 ± 49.72	123.98 ± 31.77	0.081[c]
SN	34.71 ± 14.47	43.77 ± 7.67	**0.012[c]**
ST	39.94 ± 16.02	49.02 ± 9.69	**0.025[c]**
IN	34.61 ± 9.51	46.84 ± 10.51	**< 0.001[c]**
IT	42.49 ± 9.79	50.37 ± 13.24	**0.018[c]**
4Q	37.94 ± 10.83	47.50 ± 9.36	**0.002[c]**
Implicit Time, millisec			
Central	44.06 ± 7.69	41.76 ± 2.69	0.197[c]
SN	39.57 ± 1.51	39.08 ± 1.71	0.289[c]
ST	39.84 ± 1.67	39.15 ± 1.88	0.176[c]
IN	39.25 ± 1.68	38.9 ± 1.82	0.476[c]
IT	39.37 ± 1.44	38.98 ± 1.77	0.396[c]
4Q	39.51 ± 1.44	39.03 ± 1.78	0.293[c]
	[a] Student's t-test for independent samples		
	[b] Fisher's exact test.		
	[c] Mann−Whitney U test		

Table 2
Comparisons among the P1-wave amplitudes as evaluated in the 4 quadrants in neurofibromatosis type 1 (NF1) patients and healthy controls (HC). SD: standard deviation; SN: supero-nasal; ST: supero-temporal; IN: infero-nasal; IT: infero-temporal.

	NF1 (mean ± SD) vs (mean ± SD)	p value[a]	HC (mean ± SD) vs (mean ± SD)	p value[a]
P1 Amplitude, nV/deg²				
SN vs ST	(34.71 ± 14.47) vs (39.94 ± 16.02)	**0.046**	(43.77 ± 7.67) vs (49.02 ± 9.69)	**0.006**
SN vs IN	(34.71 ± 14.47) vs (34.62 ± 9.51)	> 0.999	(43.77 ± 7.67) vs (46.84 ± 10.51)	> 0.999
SN vs IT	(34.71 ± 14.47) vs (42.49 ± 9.79)	**0.013**	(43.77 ± 7.67) vs (50.37 ± 13.24)	**0.035**
ST vs IN	(39.94 ± 16.02) vs (34.62 ± 9.51)	0.126	(49.02 ± 9.69) vs (46.84 ± 10.51)	0.335
ST vs IT	(39.94 ± 16.02) vs (42.49 ± 9.79)	0.649	(49.02 ± 9.69) vs (50.37 ± 13.24)	> 0.999
IN vs IT	(34.62 ± 9.51) vs (42.49 ± 9.79)	**< 0.001**	(46.84 ± 10.51) vs (50.37 ± 13.24)	> 0.999
	[a]Friedman test			

Discussion

The purpose of our study was to examine neuroretinal function in NF1 patients without OPGs compared to a group of HCs by the use of mfERG. The mfERG is a validated methodology for clinical evaluation of several conditions, including retinitis pigmentosa, hydroxychloroquine toxicity, glaucoma, ocular vascular occlusive disorders [22–27]. Reveling subclinical abnormalities of retinal function, mfERG can identify patients at risk of retinal damage progression allowing for early therapeutic interventions [28–31]. Currently, there are no available studies in the literature investigating the value of mfERG in NF1 patients. Limited studies demonstrated retinal electrofunctional anomalies in NF1 regardless of the presence of OPGs, although the clinical meaning of these findings is still unknown [32,33]. Lubiński et al. performed electro-oculogram (EOG) and full-field flash ERG evaluations in patients diagnosed with NF-1 and variable ocular manifestations including optic nerve gliomas (< 5%), and compared results to normal healthy controls [32,33]. These authors reported a significative increase in the Arden indexes of the EOG test in NF1 patients, whereas there were no recorded abnormalities in the flash ERG examination. The reported EOG changes were attributed to calcium level variations caused by melanin abnormalities related to reduced expression of neurofibromin [32,33].

To our knowledge, this is the first study evaluating neuroretinal function in NF1 patients in the absence of OPGs.

In our study, we identified electro functional disorders in NF1 patients consisting of P1 wave alterations. Specifically, NF1 patients showed a statistically significant reduction in the mfERG P1-wave amplitude in the 4 quadrants when compared to HC, with no recorded differences of the P1-wave amplitude in the 2 central degrees between the groups. These alterations were subclinical as the recruited patients all presented with normal or corrected to normal visual acuity and no underlying disease that could affect retinal function. Moreover, the absence of electroretinographic alterations in the 2 central retinal degrees, corresponding to the fovea centralis, reflected the absence of visual impairment in our patients.

The exact origin of the P1 wave is still debated. There is evidence that the same cellular elements that contribute to the full field ERG b-wave formation could be the source of the P1 wave. The major contribution may derive from the depolarization of bipolar cells activated by a light source. Therefore, it is believed that the b-wave is generated by cells in the inner retina [34].

There are studies showing that NF1 retinal ganglion cells (RGCs) exhibit shortened neurite length and reduced growth cone areas, with decreased survival in response to different types of injury compared to wild-type counterparts. These defective neuronal phenotypes have been suggested to reflect an abnormal neurofibromin-mediated cyclic adenosine monophosphate (cAMP) generation [35].

CAMP is a derivative of adenosine triphosphate (ATP) and serves as second messenger for intracellular signal transduction. Recently, it has been found that changes in cAMP levels have regulatory influences on the phototransduction cascade. This action exerts expanding the adaptation contingent of photoreceptors to illumination conditions, decreasing its sensitivity in bright light and increasing its sensitivity during the dark part of the day [36].

Neurofibromin is a positive regulator of cAMP levels in various cell types including neurons, and its deficit leads to a reduction in cAMP basal levels [37]. Therefore, we hypothesize that the lower levels of mfERG P1-wave amplitude in NF1 patients found in our study may be attributable to an altered intracellular signal transduction due to abnormal neurofibromin-mediated cAMP generation.

This hypothesis provides a possible biological explanation of the electrofunctional results obtained.

Moreover, the NF1 group presented a high percentage of chorioretinal alterations consisting of choroidal nodules when compared to HCs.

Variable in number and morphology, mostly located at the posterior pole, choroidal nodules are a frequent manifestation of ocular involvement in NF1 patients. These lesions represent amounts of proliferating Schwann cells, melanocytes and ganglion cells around axons of the ciliary nerves innervating the choroid [38,39]. They appear as hyperreflective-whitish lesions at SD-OCT in NIR modality, with variable features from well-defined to dull, confluent margins, according to previous evidence [40−44]. A few authors described a thinning of the overlying retinal tissue in correspondence of choroidal nodules in NF1, expression of sub-atrophy of retinal layers [45]. More recently, low flow areas overlying choroidal nodules were demonstrated at the level of choriocapillaris on OCT-angiography in a single-case report, showing topographical matching with areas of reduced chorioretinal thickness [46]. However, we are currently unable to establish any correlation between the impairment of retinal function and the presence of choroidal nodules. Further investigation aimed at evaluating choroidal nodules-related low flow to the retina and corresponding retinal functional alterations detected by the use of mfERG is encouraged.

Additional findings from our study consisted in significative differences in the mf-ERG P1-wave amplitudes in the 4 quadrants within the NF1 group, and lower amplitudes were detected in the nasal quadrants.

In HCs, we observed similar differences regarding amplitude values with lower values registered in the supero-nasal quadrant if compared to temporal quadrants (SN vs ST; SN vs IT) (Table 2).

Although lower values of amplitudes in the nasal quadrants appear to be physiological as per previous evidence [47], the significantly reduced amplitudes detectable in each quadrant of mfERG evaluation in NF1 patients compared to HC must be clarified.

The clinical significance of the recorded electro-functional abnormalities in NF1 patients remains unclear. Prospective studies are needed to evaluate long-term responses in patients with NF1 and potential correlation with progressive visual impairment. In summary, mfERG evaluation in patients affected by NF1 showed a decreased amplitude of the P1-wave between 2 and 25 central retinal degrees attributable to retinal function impairment. This abnormality is subclinical as all patients did not have a reduced visual acuity nor had any underlying disease that could have affected the outcome of the research. These observations suggest a possible use of mfERG as subclinical retinal damage indicator with a potential utility in clinical practice for the follow-up of NF1 patients.

Methods

This observational, cross sectional study was conducted at the University of Rome 'Sapienza', Umberto I Hospital, Italy, from June 2019 to February 2020. The study was prospectively reviewed by the Ethics Committee of the Sapienza University of Rome. The research followed the Tenets of the Declaration of Helsinki, and informed consent was obtained from all subjects of the study. We included 35 consecutive patients (35 eyes; 21 females and 14 males) between 18 and 55 years of age (mean age: 31 ± 10.1 years) with a diagnosis of NF1 based on the National Institutes of Health (NIH) criteria [15] and 30 healthy subjects (30 eyes; 17 females, 13 males) between 18 and 60 years of age mean age 33.30 ± 6.0 SD for control group.

Inclusion criteria were:

- Best corrected visual acuity (BCVA) not less than 20/20 in each eye;

- Refractive defects less than ± 4 D (spherical equivalent);

- Absence of OPGs and any other disorder of the visual pathways;

- Absence of ocular, systemic and/or neuroretinal pathologies that could affect retinal function;

- Absence of NF1-related manifestations at the fundus oculi examination

Exclusion criteria were:

- Poor collaboration which prevented the correct execution of diagnostic exams;

- Excessive signal-to-noise ratio, artifacts and non-uniform waveforms at mfERG.

Healthy subjects were recruited from outpatients of the eye clinic of the University of Rome 'Sapienza'.

Each subject underwent detailed clinical examination including: Snellen measurement of the BCVA, biomicroscopic examination of the anterior segment, Goldmann applanation tonometry, mydriatic indirect fundus biomicroscopy, cross-sectional spectral domain-optical coherence tomography (SD-OCT) and SD-OCT in near-infrared reflectance (NIR) modality, multifocal electroretinogram (mf-ERG) exam.

Additionally, all NF-1 patients underwent 1.5-Tesla MRI scan of the brain to assess the presence of OPGs.

SD-OCT scans were obtained with the Spectralis OCT (Spectralis Family Acquisition Module, V 5.1.6.0; Heidelberg Engineering, Heidelberg, Germany), following a standardized protocol.

The mfERG exam was performed after administration of 1% tropicamide topical solution in both eyes, followed by an adaptation to daylight for about 30 minutes. The mfERG recording was performed by using an ERG-Jet corneal contact lens active electrode under topical anesthetic solution of 0.5% benoxinate topical solution in the subject eye. The reference electrode was attached next to the corresponding outer canthus. The neutral electrode was applied with conduction gel on the patient's earlobe. The examination was performed individually for each eye for a duration of approximately 5–7 minutes, with application of a bandage on the fellow eye. Each patient was placed on the chin-guard of the visual stimulator at 33 cm from the display and was corrected with a temple lens for near vision, where required, due to the pharmacologically induced accommodative block. The stimulus was represented by a pseudorandomized sequence of alternating light and dark hexagonal flashes, with any given flash having a 50% possibility to change in each single frame [16–18]. Electrodes were connected with a junctional box from which the amplified signals were delivered to a digital recording system for graphic transformation into a path of negative and positive waves. The MfERG signals were analyzed on the computerized Optoelectronic Stimulator Vision Monitor MonPack 120 Metrovision (Perenchies, France) with reference to the International Society for Clinical Electrophysiology of Vision (ISCEV) guidelines [16]. The first order Kernel mfERG component was used to evaluate amplitude and implicit times of N1, P1, and N2 wave peaks. The areas were analyzed in quadrants from 2 to 25 degrees of eccentricity relative to fixation and the analysis generated a histogram for each of the extended zones. The analysis was carried out on 6 zones: the 2 central degrees, the 4 quadrants from 2 to 25 degrees of eccentricity, and the overall average of the 4 quadrants, for an array of 61 elements scaled with eccentricity by means of the 61 program. The analysis of mfERG data was performed in 2 steps:

- 'Analysis of the trace arrays': evaluating the shape of the wave;
- 'Group averages': evaluating the differences of the absolute values of amplitude and implicit time of P1 wave between NF1 and HC groups.

The right eye was selected for data analysis in each study subject.

The assessors were masked to whether or not the patients and controls had NF1.

Declarations

Authors' contributions

Study conception and design: AM, MN. Acquisition of data: AM, LL, MN. Analysis and interpretation of data: AM, MN, LL, VR. Drafting of manuscript: LL, FM, MM, MN, LA. Critical revision: AM, SG, MN, AL. This manuscript has been read and approved by all the authors and each author believes that the manuscript represents honest work. All authors meet the requirements for authorship and all express full consent for publication on your esteemed Journal.

Ethics Approval and Consent to Participate

All procedures performed in studies involving human participants were in accordance with the ethical standards of the institutional research committee of Sapienza University of Rome and with the 1964 Helsinki declaration and its later amendments or comparable ethical standards. Informed consent was obtained from all individual participants included in the study.

Consent for publication

Informed consent to publish personal or clinical details along with any identifying images was obtained from study patients.

Data Availability Statement

The data used to support the findings of this study are available from the corresponding author upon request.

Conflict of Interest

All authors certify that they have no financial or proprietary interest in the subject matter or materials discussed in this manuscript. The authors declare that they do not have any conflicts or potential conflicts of interest

Funding Statement

No financial support has been requested for the study.

References

1.   Anderson, J. L. & Gutmann, D. H. Neurofibromatosis type 1. in *Handbook of Clinical Neurology* vol. 132 75–86 (Elsevier B.V., 2015).

2.   Rasmussen, S. A. & Friedman, J. M. NF1 gene and neurofibromatosis 1. *American Journal of Epidemiology* vol. 151 33–40 (2000).

3.   Miraglia, E. *et al.* Cutaneous manifestations in neurofibromatosis type 1. *Clin. Ter.* **171**, e371–e377 (2020).

4.   Kinori, M., Hodgson, N. & Zeid, J. L. Ophthalmic manifestations in neurofibromatosis type 1. *Survey of Ophthalmology* vol. 63 518–533 (2018).

5.   Moramarco, A. *et al.* Retinal microvascular abnormalities in neurofibromatosis type 1. *Br. J. Ophthalmol.* **103**, 1590–1594 (2019).

6.   Moramarco, A. *et al.* Hyperpigmented spots at fundus examination: a new ocular sign in Neurofibromatosis Type I. *Orphanet J. Rare Dis.* **16**, (2021).

7.   Moramarco, A. *et al.* Ocular surface involvement in patients with neurofibromatosis type 1 syndrome. *Graefe's Arch. Clin. Exp. Ophthalmol.* **258**, 1757–1762 (2020).

8.   Cohen, M. E. & Duffner, P. K. Visual-evoked responses in children with optic gliomas, with and without neurofibromatosis. *Pediatr. Neurosurg.* **10**, 99–111 (1983).

9.   North, K., Cochineas, C., Tang, E. & Fagan, E. Optic gliomas in neurofibromatosis type 1: Role of visual evoked potentials. *Pediatr. Neurol.* **10**, 117–123 (1994).

10.	Iannaccone, A. *et al.* Visual evoked potentials in children with neurofibromatosis type 1. *Doc. Ophthalmol.* **105**, 63–81 (2002).

11.	Nebbioso, M. *et al.* Neurofibromatosis type 1: Ocular electrophysiological and perimetric anomalies. *Eye Brain* **12**, 119–127 (2020).

12.	Hegedus, B. *et al.* Optic nerve dysfunction in a mouse model of neurofibromatosis-1 optic glioma. *J. Neuropathol. Exp. Neurol.* **68**, 542–551 (2009).

13.	Abed, E. *et al.* Functional loss of the inner retina in childhood optic gliomas detected by photopic negative response. *Investig. Ophthalmol. Vis. Sci.* **56**, 2469–2474 (2015).

14.	Sutter, E. E. & Tran, D. The field topography of ERG components in man-I. The photopic luminance response. *Vision Res.* **32**, 433–446 (1992).

15.	National Institutes of Health Consensus Development Conference Statement: neurofibromatosis. Bethesda, Md., USA, July 13-15, 1987. in *Neurofibromatosis* vol. 1 172–178 (1988).

16.	Hood, D. C. *et al.* ISCEV standard for clinical multifocal electroretinography (mfERG) (2011 edition). *Doc. Ophthalmol.* **124**, 1–13 (2012).

17.	Marmor, M. F. *et al.* ISCEV Standard for full-field clinical electroretinography (2008 update). in *Documenta Ophthalmologica* vol. 118 69–77 (Doc Ophthalmol, 2009).

18.	Hoffmann, M. B. *et al.* ISCEV standard for clinical multifocal electroretinography (mfERG) (2021 update). *Doc. Ophthalmol.* **142**, 5–16 (2021).

19.	Vagge, A. *et al.* Choroidal abnormalities in neurofibromatosis type 1 detected by near-infrared reflectance imaging in paediatric population. *Acta Ophthalmol.* **93**, e667–e671 (2015).

20.	Moramarco, A. *et al.* Near-infrared imaging: an in vivo, non-invasive diagnostic tool in neurofibromatosis type 1. *Graefe's Arch. Clin. Exp. Ophthalmol.* **256**, 307–311 (2018).

21.	Moramarco, A., Giustini, S., Miraglia, E. & Sacchetti, M. SD-OCT in NIR modality to diagnose retinal microvascular abnormalities in neurofibromatosis type 1. *Graefe's Archive for Clinical and Experimental Ophthalmology* vol. 256 1789–1790 (2018).

22.	Tsang, A. C. *et al.* The Diagnostic Utility of Multifocal Electroretinography in Detecting Chloroquine and Hydroxychloroquine Retinal Toxicity. *Am. J. Ophthalmol.* **206**, 132–139 (2019).

23.	Moschos, M. M. *et al.* Correlation between optical coherence tomography and multifocal electroretinogram fndings with visual acuity in retinitis pigmentosa. *Clin. Ophthalmol.* **7**, 2073–2078 (2013).

24.	Kaneko, M., Machida, S., Hoshi, Y. & Kurosaka, D. Alterations of photopic negative response of multifocal electroretinogram in patients with glaucoma. *Curr. Eye Res.* **40**, 77–86 (2015).

25.	Nebbioso, M., Livani, M. L., Steigerwalt, R. D., Panetta, V. & Rispoli, E. Retina in rheumatic diseases: Standard full field and multifocal electroretinography in hydroxychloroquine retinal dysfunction. *Clin. Exp. Optom.* **94**, 276–283 (2011).

26.	Ohshima, A., Hasegawa, S., Takada, R., Takagi, M. & Abe, H. Multifocal electroretinograms in patients with branch retinal artery occlusion. *Jpn. J. Ophthalmol.* **45**, 516–522 (2001).

27.	Abdel-Kader, M. & El-Dessouky, W. M. Multifocal electroretinogram in retinal vein occlusion. *Saudi J. Ophthalmol.* **24**, 125–132 (2010).

28.	Lyons, J. S. & Severns, M. L. Detection of Early Hydroxychloroquine Retinal Toxicity Enhanced by Ring Ratio Analysis of Multifocal Electroretinography. *Am. J. Ophthalmol.* **143**, (2007).

29.   Dolan, F. M., Parks, S., Hammer, H. & Keating, D. The wide field multifocal electroretinogram reveals retinal dysfunction in early retinitis pigmentosa [12]. *British Journal of Ophthalmology* vol. 86 480–481 (2002).

30.   Nebbioso, M., Grenga, R. & Karavitis, P. Early detection of macular changes with multifocal ERG in patients on antimalarial drug therapy. *J. Ocul. Pharmacol. Ther.* **25**, 249–258 (2009).

31.   Gölemez, H., Yıldırım, N. & Özer, A. Is multifocal electroretinography an early predictor of glaucoma? *Doc. Ophthalmol.* **132**, 27–37 (2016).

32.   Lubiński, W. *et al.* Electro-oculogram in patients with neurofibromatosis type 1. *Doc. Ophthalmol.* **103**, 91–103 (2001).

33.   Lubiński, W. *et al.* Supernormal Electro-Oculograms in Patients with Neurofibromatosis Type 1. *Hered. Cancer Clin. Pract.* **2**, 193 (2004).

34.   Perlman I. The electroretinogram: ERG by IDO Perlman. Webvision: The Organization of the Retina and. 2015. - Search Results - PubMed. https://pubmed.ncbi.nlm.nih.gov/?term=Perlman+I.+The+electroretinogram%3A+ERG+by+IDO+Perlman.+Webvision%3A+The+Organization+of+the+Retina+and.+2015.

35.   Brown, J. A., Gianino, S. M. & Gutmann, D. H. Defective cAMP generation underlies the sensitivity of CNS neurons to neurofibromatosis-1 heterozygosity. *J. Neurosci.* **30**, 5579–5589 (2010).

36.   Astakhova, L. A., Kapitskii, S. V., Govardovskii, V. I. & Firsov, M. L. Cyclic AMP as a regulator of the phototransduction cascade. *Neuroscience and Behavioral Physiology* vol. 44 664–671 (2014).

37.   Nadim, W. D. *et al.* Physical interaction between neurofibromin and serotonin 5-HT6 receptor promotes receptor constitutive activity. *Proc. Natl. Acad. Sci. U. S. A.* **113**, 12310–12315 (2016).

38.   Kurosawa, A. & Kurosawa, H. Ovoid Bodies in Choroidal Neurofibromatosis. *Arch. Ophthalmol.* **100**, 1939–1941 (1982).

39.   Klein, R. M. & Glassman, L. Neurofibromatosis of the choroid. *American Journal of Ophthalmology* vol. 99 367–368 (1985).

40.   Abdolrahimzadeh, S. *et al.* Morphologic and vasculature features of the choroid and associated choroid-retinal thickness alterations in neurofibromatosis type 1. *Br. J. Ophthalmol.* **99**, 789–793 (2015).

41.   Ayata, A., Ünal, M., Ersanli, D. & Tatlipinar, S. Near infrared fluorescence and OCT features of choroidal abnormalities in type 1 neurofibromatosis. *Clin. Exp. Ophthalmol.* **36**, 390–392 (2008).

42.   Rao, R. C. & Choudhry, N. Enhanced depth imaging spectral-domain optical coherence tomography findings in choroidal neurofibromatosis. *Ophthalmic Surg. Lasers Imaging Retin.* **45**, 466–468 (2014).

43.   Ueda-Consolvo, T., Miyakoshi, A., Ozaki, H., Houki, S. & Hayashi, A. Near-infrared fundus autofluorescence-visualized melanin in the choroidal abnormalities of neurofibromatosis type 1. *Clin. Ophthalmol.* **6**, 1191–1194 (2012).

44.   Byun, Y. S. & Park, Y. H. Indocyanine green angiographic findings of obscure choroidal abnormalities in neurofibromatosis. *Korean J. Ophthalmol.* **26**, 230–234 (2012).

45.   Abdolrahimzadeh, S. *et al.* Retinal microvascular abnormalities overlying choroidal nodules in neurofibromatosis type 1. *BMC Ophthalmol.* **14**, (2014).

46.   Kumar, V. & Singh, S. Multimodal imaging of choroidal nodules in neurofibromatosis type-1. *Indian J. Ophthalmol.* **66**, 586–588 (2018).

47.   Hood, D. C. Assessing retinal function with the multifocal technique. *Progress in Retinal and Eye Research* vol. 19 607–646 (2000).
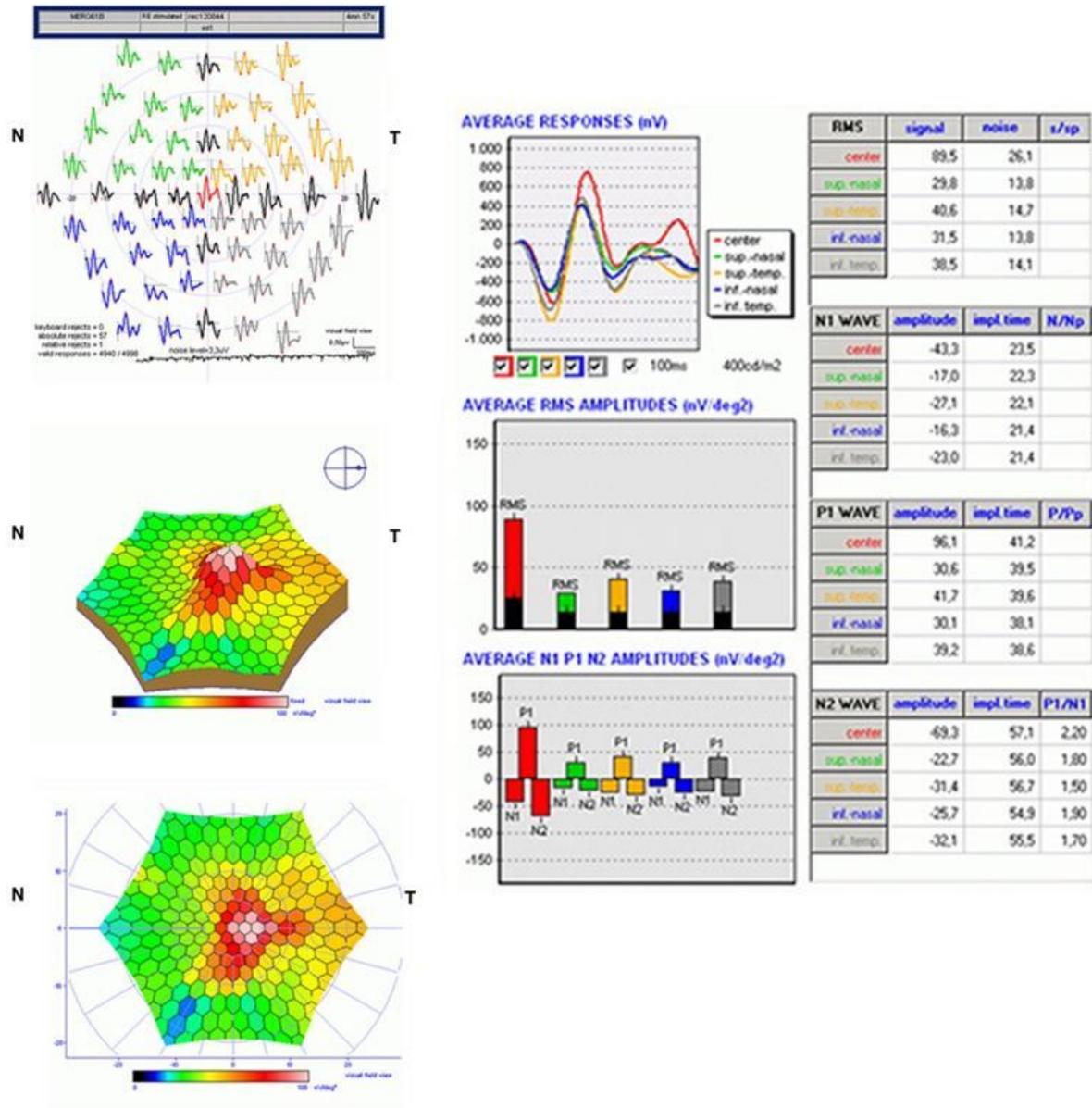
Figures

Figure 1

Multifocal electroretinogram (MfERG) of NF1 patient (V.S.). Average values of amplitude and implicit time within 2 central degrees and in the 4 quadrants examined (right panel). Wave traces and three-dimensional and one-dimensional representation (left panel). Note in the right panel the average values of the amplitudes of the P1 wave and the corresponding histograms with reduced amplitude at the level of the nasal quadrants (superior 30.6nV/deg2 with histogram in green, and inferior 30.1nV/deg2 with histogram in blue) compared to the temporal ones (superior 41.7nV/deg2 with histogram in yellow, and inferior 39.2nV/deg2 with histogram in gray).
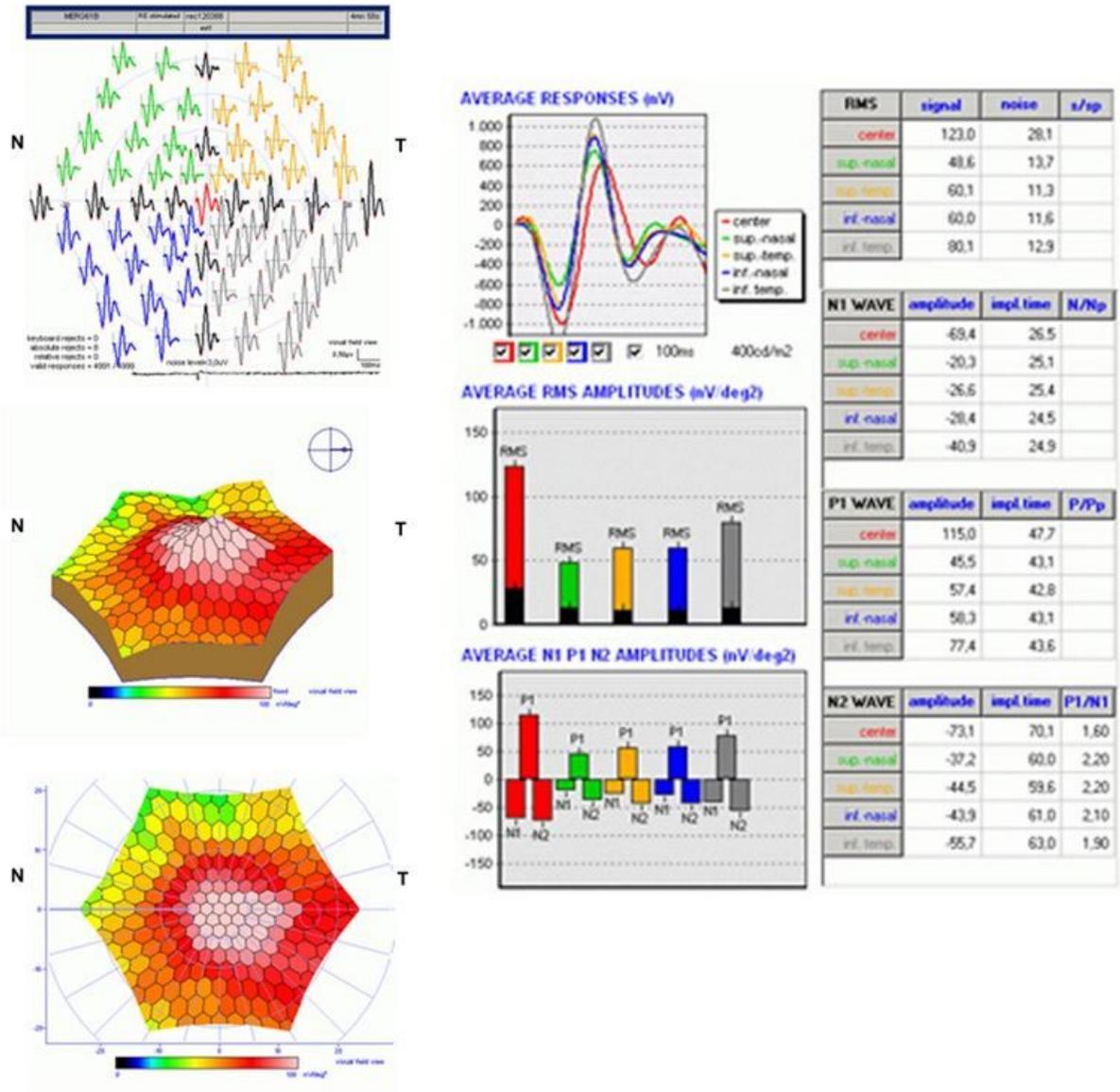
Figure 2

Multifocal electroretinogram (MfERG) of control subject (M.R.). Average values for amplitude and implicit time in the 2 central degrees and in the 4 quadrants examined (right panel). Wave traces and three-dimensional and one-dimensional representation (left panel). Note in the right panel the average values of the P1 wave amplitudes and the histograms corresponding to the various quadrants with lower amplitude (45.5 nV/deg2) at the level of the nasal-superior quadrant (green histogram).
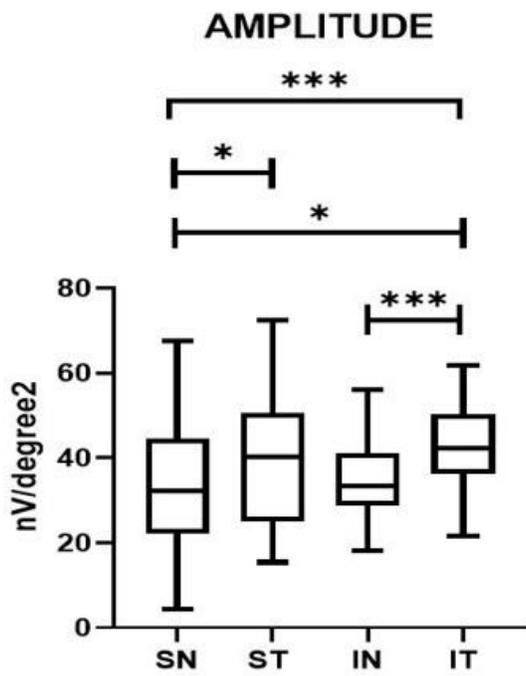
Figure 3

Mean values of amplitudes in the different retinal regions of neurofibromatosis type 1 (NF1) patients. * p<0.01; *** p <0.001; SN: supero-nasal; ST: supero-temporal; IN: infero-nasal; IT: infero-temporal.